Reconstruction of Tsunami Occurrence on Okushiri Island, Southwestern Hokkaido, Japan

Atsushi Urabe (urabe@gs.niigata-u.ac.jp)
Niigata University https://orcid.org/0000-0002-8361-9794
Yoshihiro Kase
Geological Survey of Hokkaido
Gentaro Kawakami
Hokkaido Prefecture: Hokkaido
Kenji Nishina
Hokkaido Prefecture: Hokkaido
Yasuhiro Takashimizu
Niigata Daigaku - Igarashi Campus: Niigata Daigaku
Hiroyuki Miyazawa
tolex
Fumika Hirano
Tohoku University: Tohoku Daigaku

Full paper

Keywords: tsunami deposit, tsunami recurrence, Okushiri Island, Hokkaido, Japan Sea

Posted Date: October 12th, 2021

DOI: https://doi.org/10.21203/rs.3.rs-951436/v1

Reconstruction of tsunami occurrence on Okushiri Island, southwestern Hokkaido, Japan

Atsushi Urabe*

Research Institute for Natural Hazards and Disaster Recovery, Niigata University, Ikarashi 2-8050, Nishi-ku, Niigata, Japan, 950-2181, urabe@gs.niigata-u.ac.jp

* corresponding author

Yoshihiro Kase

Geological Survey of Hokkaido, Hokkaido Research Organization, Kita 19, Nishi 11, Kita-Ku, Sapporo, Japan, 060-0819, kase-yoshihiro@hro.or.jp

Gentaro Kawakami

Geological Survey of Hokkaido, Hokkaido Research Organization, Kita 19, Nishi 11, Kita-Ku, Sapporo, Japan, 060-0819, kawakami-gentaro@hro.or.jp

17 Kenji Nishina

18 Geological Survey of Hokkaido, Hokkaido Research Organization, Kita 19, Nishi 11,

19 Kita-Ku, Sapporo, Japan, 060-0819, nishina-kenji@hro.or.jp

20

21 Yasuhiro Takashimizu

22 Mathematical and Natural Sciences Course, Faculty of Education, Institute of Humanities,

23 Social Sciences and Education, Niigata University, Ikarashi 2-8050, Nishi-ku, Niigata,

24 Japan, 950-2181, takashimi@ed.niigata-u.ac.jp

25

26 Hiroyuki Miyazawa

27 Higashi-Nihon Sogo Keikaku Co.,Ltd, Narihira 3-14-4, Sumida-ku, Tokyo, Japan, 130-

28 0002, miyazawah@tolex.co.jp

29

30 Fumika Hirano

31 Department of Earth Science, Graduate School of Science, Tohoku University, Aoba 468-

32 1, Aramaki, Aoba-ku, Sendai, Japan, 980-8572, hirano.fumika.t7@dc.tohoku.ac.jp

33

34 **Indicate the corresponding author**

35 Atsushi Urabe, urabe@gs.niigata-u.ac.jp

Abstract

The eastern margin of the Japan Sea is located along an active convergent boundary between the North American and Eurasian tectonic plates. Okushiri Island, which is situated off the southwest coast of Hokkaido, is located in an active tectonic zone where many active submarine faults are distributed. Studying the records of past tsunamis on Okushiri Island is important for reconstructing the history and frequency of fault activity in this region, as well as the history of tsunamis in the northern part of the eastern margin of the Japan Sea. Five tsunami deposit horizons have been identified previously on Okushiri Island, including that of the 1741 tsunami, which are interbedded in the coastal lowlands and Holocene terraces. However, these known tsunami deposits date back only ~3,000 years. A much longer record of tsunami occurrence is required to consider the frequency of submarine fault activity. In this study, we cored from 7 to 25 m depth in the Wasabiyachi lowland on the southern part of Okushiri Island, where previous studies have confirmed the presence of multiple tsunami deposits on peat layer surfaces. The results indicate that the Wasabiyachi lowland comprises an area that was obstructed by coastal barriers between the lowland and the coast at ~8.5 ka and consists of muddy

sediment and peat layers formed in lagoons and floodplains, respectively. In addition, event deposits and 15 tsunami horizons were observed among the turbidites and peat layers, dating back as far as 3,000 years. Combined with previous findings, Okushiri Island has sustained 20 tsunami events between ~7.5 ka and the present. These findings are critical for investigating the activities of submarine faults off the southwestern coast of Hokkaido, as well as for determining tsunami risks along the coast of the Japan Sea between North Tohoku and Hokkaido.

Keywords

tsunami deposit, tsunami recurrence, Okushiri Island, Hokkaido, Japan Sea

Main Text

1. Introduction

The 2011 Tohoku-Oki earthquake produced a tsunami that caused severe damage to the Pacific coast of the Tohoku region (Japan Meteorological Agency, 2012). Following the tsunami disaster, local governments along the coast of the Japan Sea have

68 evaluated their tsunami risks by predicting tsunami heights in each region and by
69 reconstructing tsunami occurrence histories. In recent years, tsunamis in the Japan Sea
70 caused by the 1983 Middle Japan Sea earthquake, and the 1993 Hokkaido Nansei-Oki
71 earthquake have caused severe damage (Fig. 1). Among these, the 1983 Middle Japan
72 Sea earthquake (Mj=7.7, Mw=7.7) that occurred off the coast of the Tsugaru region of
73 Aomori Prefecture produced a tsunami with high watermarks of over 10 m in the coastal
74 area that extended from Happo Town to the right bank of the Yoneshiro River in Akita
75 Prefecture, with a maximum upstream height of 14.9 m in Minehama, Happo Town.
76 Tsunamis have claimed over 100 lives in Akita and Aomori Prefectures（Japan
77 Meteorological Agency, 1984, Aomori Prefecture, 1984; Shuto, 1984; Abe and Ishii,
78 1987）. The 1993 Hokkaido Nansei-Oki earthquake (Mj=7.8, Mw=7.7) occurred off the
79 northwest coast of Okushiri Island, Hokkaido. High watermarks on Okushiri Island from
80 the tsunami were 10–20 m or higher at some locations. At Aonae, located at the southern
81 end of Okushiri Island, the tsunami arrived from the west and traveled northeast, with
82 maximum heights of more than 7–10 m. As a result, 198 lives were lost on Okushiri Island,
83 of which 109 were victims of the tsunami in the Aonae district（Geological Survey of

84 Hokkaido, 1994; Japan Meteorological Agency, 1995）.

85 As the tsunami risks along the coast of the Japan Sea are currently being re-
86 evaluated, the Committee for Technical Investigation on Large-Scale Earthquakes in the
87 Sea of Japan (2014) (hereafter abbreviated as the Committee of the Japan Sea) has
88 summarized the distribution of active submarine faults throughout the Japan Sea and
89 created a rectangular model of tsunami sources based on previously collected seafloor
90 geophysical data. Moreover, data relating to tsunamis produced by historical earthquakes
91 in the Japan Sea and research on tsunami deposits were compiled and assessed to
92 reconstruct the historical record of tsunamis for each region (Committee of the Japan Sea,
93 2014). Furthermore, local governments along the coast of the Japan Sea have estimated
94 the local tsunami inundation, the tsunami risk for each region, and potential damage based
95 on tentative modeling. However, compared to the Pacific coast, there are fewer historical
96 records of earthquakes and tsunamis along the coast of the Japan Sea, making it difficult
97 to clarify tsunami occurrence in the Japan Sea that can serve as a basis for tsunami risk
98 evaluation.

99 Accordingly, tsunami occurrences have been investigated using deposits not

100 only along the coast of the Japan Sea, but also further off the Pacific coast of the Tohoku
101 region. However, reconstructing past tsunami occurrences, including events prior to 2011,
102 have been limited to tsunamis that occurred ~2–3 ka (Minoura et al., 1987; Minoura and
103 Nakaya, 1990, 1991; Nanayama et al, 2000; Nishimura et al., 1999; Nishimura et al.,
104 2000; Kamataki et al., 2015, 2016, 2017, 2018a, b, 2019; Kase et al., 2016; Kawakami et
105 al., 2015; Okada et al., 2018, 2019). Because the period between events is short in terms
106 of the frequency of fault activity along the coast of the Japan Sea (approximately once
107 every few thousand years), it is necessary to investigate strata that date beyond a few
108 thousand years ago in addition to widely distributed tsunami deposits (Kawakami et al.,
109 2017b; Urabe, 2019; Takashimizu et al., 2020).

110 In this study, we investigated the Wasabiyachi lowland at the southern end of
111 Okushiri Island, Hokkaido, to observe and analyze tsunami occurrences between
112 Hokkaido and the North Tohoku coast prior to a few thousand years ago. The
113 Wasabiyachi River has a small drainage area that flows into Aonae Bay. Peat layers were
114 deposited on the surface of the Wasabiyachi lowland. According to Kase et al. (2016) and
115 Kawakami et al. (2017a, b), these peat layers (~0–2 m depth) include four to five

116 interbedded medium-grained sand layers that exhibit erosive bases and weak normally
117 graded structures. These sand layers have been determined to be tsunami-induced
118 deposits based on landward changes in grain size and layer thickness, as well as owing to
119 the paleocurrent, distribution, and characteristics of microfossils in the sand layers. The
120 estimated ages of the tsunami deposits observed on Okushiri Island are 1741 C.E., 0.8–
121 0.9 ka, 1.5–1.6 ka, 2.4–2.6 ka, and 2.8–3.1 ka (Kawakami et al. 2017a, b).

122 Accordingly, we cored from 7 to 25 m at five of the sites surveyed by Kase et
123 al. (2016) and Kawakami et al. (2017a, b) to examine tsunami-generated deposits older
124 than 3 ka. We identified event deposits related to 20 tsunami horizons, dating back to ~7
125 ka, including the five tsunami deposits reported by Kase et al. (2016). This constitutes the
126 first reconstruction of tsunami occurrence along the coast of the Japan Sea off
127 southwestern Hokkaido. These findings are important for further extended
128 reconstructions of tsunamis in the Japan Sea from the coast of Niigata Prefecture to North
129 Tohoku.

130

131 ------Figure 1------

2. Geologic and topographic setting

2.1. Okushiri Island

The area between the coastal region along the Japan Sea side of northeastern Japan contains many reverse faults and is known as the Japan Sea Eastern Margin Mobile Belt (Taira, 2002). The eastern margin of the northern Japan Sea is located at the boundary between the North American and Eurasian (Amurian) tectonic plates (Seno et al., 1996; Isozaki et al., 2010), and a compressive stress field has developed in this region (Seno, 1999; Okamura, 2000). Therefore, many active onshore and submarine faults are located within a short distance (~200–250 km) from the coast to the offshore area of the northern Tohoku to Hokkaido region (Fig. 1).

Okushiri Island is located on Okushiri Ridge, which extends N–S in the northern part of the Japan Sea Eastern Margin Mobile Belt. Previous studies have shown that many active submarine faults are located around Okushiri Island. These faults originally contributed to the expansion of the Japan Sea as normal faults, but have been reactivated as reverse faults since the Quaternary (Okamura, 2010). The Committee of

148 the Japan Sea (2014) investigated the continuities of active submarine faults that could
149 act as the source of a tsunami based on existing geological surveys of the seafloor and
150 obtained a rectangular model for the tsunami source faults. Tsunami source faults
151 between F06 and F24 were observed in the offshore regions extending from North
152 Tohoku to Hokkaido, which includes Okushiri Island. Among these faults is the
153 epicentral area of the 1993 Hokkaido Nansei-Oki earthquake, which is located northwest
154 of Okushiri Island (Fig. 1).
155
156 **2.2. Wasabiyachi lowland**
157 Okushiri Island has a long N‐S trapezoidal shape with a perimeter of 84 km.
158 The Wasabiyachi lowland is located north of the Aonae district at the southern end of
159 Okushiri Island. The Wasabiyachi lowland is a narrow lowland area, with a depth of ~2
160 km and a width of 50–500 m and surrounded by an MIS 5c marine terrace that has an
161 elevation of 20–30 m（Fig. 2; Miyoshi et al.， 1985）. The base of the marine terrace
162 consists of marine mudstones and sandstones of Miocene to Neogene age (Miyoshi et al.,
163 1985).

All of the coring sites were located on grassland (former paddy fields) at an elevation of 5 m and located ~300–500 m from the present coastline. The Aonae coastal sand dunes have an elevation of ~10 m and occur along the present coast of the Wasabiyachi River estuary（Hokkaido archaeological operations center, 2002). A beach ridge comprising ~5 m thick sand layers is located up to ~100 m landward of the sand dunes along the coast. Thus, the Wasabiyachi lowland is located in a topographic setting that is separated from the coast by sand dunes and a sandy beach ridge (Fig. 2). Further, the tidal level in Aonae at the southern end of Okushiri Island is ~40 cm at high tide. The tidal difference at Aonae is ~20 cm.

------Figure 2------

3. Materials and methods

3.1. Borehole sampling

Using a hand corer and excavating two pits, Kase et al. (2016) examined tsunami deposits in the surface layer (peat layer) of the Wasabiyachi lowland to 2–2.5 m

depths. Their results clarified the distributions of several layered tsunami deposits with ages of up to ~3,000 ka. In this study, we investigated deeper depths to observe tsunami records with ages of up to ~7,000-8,000 ka. A rotary corer and a rotating vibrational corer were used for the excavations. Each core had an internal diameter of 86 mm. Five core excavations were made (sites OKU-1–OKU-5). Site OKU-1 (42°4'3.70" N, 139°27'2.86" E, elevation 5.0 m) was located near the coast in the lowlands. Site OKU-2 (42°4'4.60" N, 139°26'59.38" E, elevation 4.9 m) is in the vicinity of the trial pit made by Kase et al. (2016). Site OKU-3 (42°4'6.80" N, 139°27'59.38" E, elevation 5.0 m) is located at the center of the lowland area. Sites OKU-4 (42°4'8.86" N, 139°26'59.77" E, elevation 5.2 m) and OKU-5 (42°4'10.29" N, 139°27'0.89" E, elevation 5.2 m) were located further inland (Fig. 2). The lengths of the cores collected from sites OKU-1 to OKU-5 were 23 m, 7 m, 25 m, 17 m, and 10 m, respectively. The OKU-1 and OKU-2 cores extended beyond the alluvium that constitutes the lowland strata and reached bedrock (Fig. 3).

3.2. Core analyses

The core samples were halved and the depositional facies were described and

196 photographed. Samples were collected for grain size and total sulfur (TS) analyses, as
197 well as dating.

198 Samples were collected for grain size analysis every 0.5 cm in the thinly
199 laminated clay layer, every 1 cm in the silt layer, and every 1 cm in the sand layers in the
200 OKU-1 and OKU-3 cores. Samples were also collected every 1 cm in the sand layers in
201 the OKU-2, OKU-4, and OKU-5 cores. Samples were not collected from the humus layers
202 in any of the cores. The samples were pre-treated with a 10% hydrogen peroxide solution
203 to remove organic matter. Grain sizes were measured using a Mastersizer 3000 laser
204 diffraction-type grain size analyzer (Malvern Panalytical Ltd.).

205 The samples used for total sulfur analyses were muddy sediments from the
206 OKU-2 core (2.6–20.0 m depth) at intervals of 20 cm and with a sample thickness of 1
207 cm. The samples were analyzed using an EMIA-120 sulfur analyzer (Horiba Ltd.).

208 Plant fragments were dated to obtain the corresponding layer ages using
209 accelerator mass spectrometry (AMS) at the Accelerator Mass Spectrometry Co., Ltd.
210 (Shirakawa City, Fukushima Prefecture). The IntCal 20 (Reimer et al., 2020) database of
211 plant fragments and peaty samples and the OxCal v4.4.2 calibration program (Bronk

212 Ramsey, 2009) were used to calculate the calibrated ages (Table 1). As a reference, two
213 samples were also dated (at Accelerator Mass Spectrometry Co. Ltd.) using shell pieces
214 and the data were corrected using a Marine 20 (Heaton et al., 2020) database (Table 1).
215 In addition, we also recalculated the calibrated radiocarbon ages of eight
216 samples collected by Kase et al. (2016) from the Wasabiyachi lowland using the IntCal
217 20 database and the OxCal v4.4.2 calibration program (Table 2).
218
219 ------Table 1 and Table 2------
220
221 **4. Results**
222 **4.1. Depositional facies**
223 The OKU-1 and OKU-5 cores were divided into eight depositional facies,
224 excluding the uppermost topsoil and the basement bedrock (Fig. 3). In addition, well-
225 sorted sand layers, which indicate a depositional process that is distinctly different from
226 that of the regular depositional environment, were recorded separately as event deposits.
227 **4.1.1. Facies FL1**

A gravelly facies was observed in the lower layers of three cores (OKU-1: 16.0–21.2 m depth, OKU-3: 20.0–25.0 m depth, OKU-4: 16.0–17.0 m depth). This depositional facies comprises a fine to medium-grained gravel layer and a partially organic silt layer. The gravel is poorly sorted and contains many light gray to green-gray silty gravel that originated from the bedrock. The matrix of the gravel layer consists of gray sandy silt and poorly sorted fine to medium-grained sand. The organic sandy silt layer includes poorly sorted silty gravel of granule size.

4.1.2. Facies FL2

This facies was observed in the lower part of two cores (OKU-3: 16.5–20.0 m depth, OKU-4: 14.6–16.0 m depth). It consists of a slightly poorly sorted organic sandy silt layer that is interbedded with a poorly sorted fine to medium-grained sand layer with a thickness of ~3–5 cm. The sandy silt layer may also contain a large amount of organic matter and may be interbedded with a thin layer of organic matter. In addition, the upper part of this facies consists of a ~50 cm thick poorly sorted sandy silt layer, including silty gravel with a granule to fine pebble size.

4.1.3. Facies FL3

244 A silty facies was observed in the upper part of three cores (OKU-2: 4.5–6.2 m
245 depth, OKU-3: 3.0–5.0 m depth, OKU-4: 3.0–5.0 m depth). This facies consists of a
246 gray–brown organic silt layer and a gray silt to sandy silt layer, wherein the bottom of the
247 gray silt to sandy silt layer is interbedded with a thin layer of clayey silt.

248 **4.1.4. Facies FL4**

249 A peaty facies was observed in the upper part of all cores (OKU-1: 1.0–4.2 m
250 depth, OKU-2: 0.9–4.5 m depth, OKU-3: 0.7–3.0 m depth, OKU-4: 0.5–3.0 m depth,
251 OKU-5: 1.8–6.0 m depth). This facies consists of an upper dark brown peat layer and a
252 lower dark brown to light brown organic silt layer. This facies also includes
253 undecomposed plant material. No bioturbation was observed.

254 **4.1.5. Facies FL5**

255 A silty was observed in the most upper parts of all cores (OKU-1: 0.4–1.0 m
256 depth, OKU-2: 0.5–0.9 m depth, OKU-3: 0.2–0.7 m depth, OKU-4: 0.2–0.5 m depth,
257 OKU-5: 0.3–1.8 m depth). This facies consists of a light brown to gray silt layer that
258 contains plant matter, and a sandy silt layer. In core OKU-5, this facies is interbedded
259 with a poorly sorted medium to coarse-grained sand layer with a thickness of 3–7 cm. No

bioturbation was observed.

4.1.6. Facies LG1

This facies was observed in the middle upper part of two cores (OKU-4: 5.2-6.2 and 12.9-14.5 m depth, OKU-5: 8.3-10.0 m depth). This facies consists of alternating gray silt and clayey silt layers. Only a small amount of bioturbation was observed. Some thin laminated layers were observed.

4.1.7. Facies LG2

This facies was observed in the middle upper part of four cores (OKU-1: 4.2-6.8 and 14.4-16.0 m depth, OKU-3: 5.0-10.8 and 13.8-16.5 m depth, OKU-4: 6.2-11.0 m depth, OKU-5: 6.0-8.3 m depth). This facies consists of a clayey silt layer in which a ~1 mm dark gray extremely fine-grained thinly laminated layer was observed, and is interbedded with a thin layer of clay or clayey silt with a thickness of < 5 cm.

4.1.8. Facies LG3

This facies was observed in the middle upper part of core OKU-3 (10.8-13.8 m depth). This facies consists of a clayey silt to clay layer in which a ~1 mm dark gray extremely fine-grained thinly laminated layer was observed.

4.1.9. Facies BA1

This facies was observed in the middle upper part of core OKU-1 (6.8–14.4 m depth). This facies consists of a well-sorted dark gray coarse to fine-grained sand layer with cross-bedding. The facies also has horizons that contain large amounts of light brown to gray silty gravel of granule to fine pebble size. This facies did not contain plant material.

-------Figure 3------

4.3. Changes in grain size and total sulfur content in core OKU-3

We measured the total sulfur content and grain size of the muddy sediment in core OKU-3, collected from the center of the Wasabiyachi lowland, to clarify any changes in the depositional environment, while excluding the gravelly facies near the basement and the humus layer at the top. The median grain size (Md), geometric mean grain size (GM), mode grain size (Mo), and geometric standard deviation (Sorting) obtained from the grain size analysis are shown in Figure 4. The Md and Sorting characteristics are described below.

292 Md sizes of 10-40 μm were observed at depths of 16.5-20.0 m (FL2). Fine
293 grains of 10-20 μm were observed at depths of 13.8-16.5 m (LG2). Slight variations of
294 10-30 μm were observed at depths of 10.8-13.8 m (LG3). Slight variations of 10-40
295 μm were observed at depths of 5.0–10.8 m (LG2), except for the sand layer. Sizes of
296 10–70 μm were observed at depths of 3.0–5.0 m (FL4), in which large size variations
297 were observed (Fig. 4).
298 A Sorting of 3.3–4.5 was observed at depths of 16.5–20.0 m (FL2). A Sorting
299 of 3.0–4.0 (max 4.8) was mainly observed at depths of 13.8–16.5 m (LG2). Variations of
300 2.8–5.8 were observed at depths of 10.8–13.8 m (LG3). Slight variations of 3.3–4.8 were
301 observed at depths of 5.0–10.8 m (LG2), except for the sand layer. A Sorting of 3.4–4.5
302 was observed at depths of 3.0–5.0 m (FL4; Fig. 4). The Md and Sorting values of the
303 event deposits in cores OKU-1 through OKU-5 are described in section 4.3.
304 SO_4^{2-} in water becomes H_2S owing to the action of sulfate-reducing bacteria
305 and is solidified in sediments as FeS_2 (via FeS). Accordingly, the total sulfur content of
306 the sediment indicates the contribution of seawater to a body of water, as well as the
307 reducing capacity of the depositional environment. Core OKU-3 had a total sulfur content

of ~0.5 wt.% at depths of 16.5–20.0 m (FL2). While variations were observed, at depths of 13.8–16.5 m (LG2) the total sulfur content was ~2.0 wt.%. At depths of 10.8–13.8 m (LG3), the total sulfur content was ~3.0 wt.%. At depths of 5.0–10.8 m (LG2), the lower and upper portions had total sulfur contents of 5.0 wt.% and 2.0 wt.%, respectively. At depths of 3.0–5.0 m (FL4), the total sulfur content varied from 0.8 to 4.0 wt.%. The results indicate an overall total sulfur content of ~0.5% between the deepest section and 16.5 m, excluding the data at 17.1 m (Fig. 4).

-------Figure 4------

4.2. Core sample age model

The radiocarbon ages of a total of 50 core samples were determined using plant material, peaty sediment, and shell fragments (Table 1). All of the radiocarbon ages conformed to the stratigraphic succession of each core. The ages of the horizons in each core were estimated based on the interval sedimentation rates and the horizons for which radiocarbon ages were obtained. Sedimentation rates were calculated for the upper and

lower ranges of the calibrated ages (2σ). The thicknesses of the event deposits were excluded from the interval sedimentation rate calculations because their deposition occurred rapidly (Fig. 5).

-------Figure 5 ------

4.3. Event deposits

The sand layers observed in all cores were interbedded with the peaty layers and muddy sediment, except for the gravel observed at the bottom of the cores (Figs. 3 and 4). A distinct boundary was also observed between the upper and lower facies of the sand layers. This indicates that the sand layers were formed by a process different from the typical depositional process in this environment. In this study, we defined an event deposit as sediment with multiple characteristic facies, including basal erosion, abrupt changes in grain size or degree of sorting, contamination with heterogeneous particles such as plant fragments or mud clasts, and containing sedimentary structures such as parallel or cross-lamination (Table 3).

In core OKU-1, which was located closest to the coast, 16 event deposit horizons were observed to a depth of 6.0 m (Fig. 3; Table 3). The upper three horizons were fine to very fine-grained or fine to medium-grained sand layers with thicknesses of 10–40 mm, while the lower horizons were well-sorted coarse to medium-grained sand layers with thicknesses of 100 mm to more than 300 mm. Core OKU-2 had a shallower bedrock depth compared to the other sites, with an alluvium thickness of ~6.2 m. Thirteen event deposit horizons were observed in this core. While these event deposits included some sand layers with thicknesses of 100 mm at horizons < 2.0 m deep, they consisted of well-sorted fine to medium-grained sand layers with thicknesses of ~5–20 mm. Some thin (7–50 mm) layers were observed at horizons deeper than 2.0 m, but these were composed of well-sorted fine to medium-grained sand layers with thicknesses of 150–340 mm (Fig. 3; Table 3). Fourteen event deposit horizons were observed in core OKU-3. While these event deposits were composed of well-sorted medium-grained sand layers with thicknesses of 4–30 mm, the horizons observed at depths of 7.79–10.4 m were interbedded with a thick (270–1,400 mm) medium-grained sand layer (Figs. 3,4 and 6 ; Table 3). Eight event deposit horizons were observed in core OKU-4. These event

356 deposits were composed of well-sorted medium-grained sand layers with thicknesses of
357 4–210 mm, the horizons observed at depths of 8.0–8.7 m were interbedded with a coarse
358 to medium-grained sand layer with a thickness of 600 mm (Fig. 3; Table 3). Ten event
359 deposit horizons were observed in core OKU-5, which was the site located furthest inland.
360 While these event deposits were interbedded with well-sorted medium to coarse-grained
361 sand layers with thicknesses of 20–190 mm, the horizons at depths of 8.6–9.3 m were
362 interbedded with a well-sorted medium to coarse-grained sand layer with a thickness of
363 600 mm (Fig. 3; Table 3).
364
365 ----- Figure 6 ------
366
367 **5. Discussion**
368 **5.1. Depositional environments**
369 Facies FL1 consists of very poorly sorted granule to fine pebble layers and
370 slightly sandy silt layers. The organic sandy silt layers also include silty gravel with a fine
371 gravel size, and are poorly sorted. Facies FL2 consists of slightly poorly sorted sandy silt

layers and is interbedded with a thin layer of poorly sorted fine to medium-grained sand layers. The sandy silt layer contains large amounts of organic matter. These poorly sorted gravel deposits, silty gravel, and turbidites that contain organic material indicate a depositional environment that was affected by fluvial processes. Intercalated silty and coarse sand layers indicate that deposition occurred in a small river channel and floodplain. The facies succession and sedimentary features indicate that facies FL1 and FL2 represent a fluvial depositional environment (Miall, 1992).

Facies FL3 consists of organic silt and sandy silt layers, while facies FL4 comprises organic silt and peat layers that contain undecomposed plant material. No bioturbation was observed in either of these facies. Organic turbidites with no observed bioturbation and peaty layers containing undecomposed plant material are indicative of a freshwater swamp environment (Miall, 1992). In both of these facies, it is possible that the fluvial channels were undeveloped swamps, as these facies did not include interbedded sand layers.

Facies FL5 consists of silt layers that contain plant material and sandy silt layers, and is interbedded with poorly sorted coarse-grained sand layers at the landward sites. As

388 no bioturbation was observed and the facies contained thin layers of coarse-grained sand,
389 this depositional facies represents a small fluvial channel and floodplain depositional
390 environment (Miall, 1992).

391 The total sulfur content of the turbidites in facies FL2 and FL3 in core OKU-3
392 were < 1 wt% (Fig. 4), indicating a non-reducing depositional environment that was not
393 affected by seawater. The depositional environment determined from the depositional
394 facies is consistent with implications of the total sulfur content.

395 Facies LG1–LG3 consist of thinly laminated clayey silt and silt layers. The
396 thinly laminated layers in LG2 and LG3 represent a typical lake environment where
397 surface disturbances do not extend to the bottom of the lake. The lack of bioturbation and
398 burrows also indicates a closed and reducing environment (Strum, 1979). LG2, which
399 contained a particularly thinly laminated interval, suggests that reducing conditions
400 persisted at the bottom. LG1 also contained silt, but some bioturbation was also observed.
401 This suggests that the water depth decreased and the number of aquatic organisms
402 increased. The succession and sedimentary features of these facies indicate a coastal
403 lagoon depositional environment. These facies also provide evidence for the

development of a coastal sand barrier that separated the Japan Sea (Aonae Bay) from an inland lagoon.

Facies BA1 consists of well-sorted coarse to fine-grained sandy layers that contain cross-bedding structures. Well-sorted sand layers indicate a depositional environment that was strongly affected by a wave environment (Reinson, 1984). Beach ridges that include sand dunes and ridges are located between the current Wasabiyachi lowland and the Japan Sea, thereby blocking the Wasabiyachi lowland estuary. Because of the differences between the depositional facies of the current environment and that of the inland lagoon environment, BA1 may represent the coastal sand barrier depositional environment.

5.2. Wasabiyachi lowland depositional processes

We investigated the alluvium formation in the Wasabiyachi lowland based on changes in the depositional facies and sediment ages in the cores. At the OKU-2 site, bedrock was reached at 6.2 m. Meanwhile, the bases of the alluvium aggrading the lowlands at sites OKU-1, OKU-3, and OKU-4 can be estimated as over 20–25 m deep.

Thus, the valley formation of the Wasabiyachi lowland occurred near sites OKU-1 through OKU-5 (Fig. 3). Fluvial material containing coarse gravel deposits (FL1 and FL2) were deposited ~9.5 ka. As sea level increased since the last glacial period near the Japanese archipelago, sites OKU-1, -3, and -4 changed rapidly to a lagoon environment, suggesting the presence of brackish water 8.5 ka. Moreover, as deposits that indicate a lagoon environment were obstructed in horizons at 14.4–16.0 m deep in core OKU-1, it is possible that a coastal barrier had already formed seaward of the surveyed area (Fig. 3). Since then, the obstructed lagoon environment expanded landward until ~5.700 ka at the OKU-5 site in the valley, and until ~5.2 ka at the seaward OKU-1 site. The depositional environment of this lagoon had a total sulfur content of 2–5 wt.% in the deposits, indicating that it was heavily obstructed and hosted a strongly reducing environment. Facies LG3 (~7–7.3 ka) was observed at depths of 11.0–14.0 m in core OKU-3 (Figs. 3 and 4). This indicates that the lagoon environment was at its most closed at ~7–7.3 ka. Moreover, the change in lagoon facies (from LG1 to LG3) indicates the early stages of lagoon formation, the progression of aggradation, and the differences in lagoon water depths from seaward to landward.

436 Based on the facies observed in core OKU-1, the coastal barrier of the
437 Wasabiyachi lowland (estuary) was estimated to have formed ~8.5 ka. Furthermore, due
438 to the observed barrier deposits at depths of 6.8–14.4 m in core OKU-1, the estuary
439 barriers can be estimated to have developed at ~6–7.5 ka, then moved seaward thereafter
440 (Fig. 3).

441 At ~5.2 ka, aggradation of the entire lagoon progressed, altering the lagoon into
442 a freshwater-affected floodplain lowland (FL3) and a lowland with peat development.
443 Since 2 ka, the peaty lowlands have been altered to slightly dry land on the inland side
444 (and at some sites), and have become fluvial floodplains.

445 Accordingly, using inferences from facies changes in the cores and the current
446 topographic environment, the Wasabiyachi lowland is a depositional environment that
447 has been obstructed by coastal barriers in the estuaries from ~8.5 ka until the present. The
448 deposits of this obstructed depositional environment are interbedded with deposits (sand
449 layers) that suggest the events described above.

450

451 **5.3. Event deposit ages, correlations, and facies changes**

452 At the study sites, the facies interbedded with event deposits were obstructed lagoons,
453 muddy floodplains, and peat deposits. We determined the ages (age ranges) of the bases
454 of the event deposits observed in each core (Table 3), assuming that the sedimentation
455 rate for each of these facies was generally constant. Among these, the sedimentary ages
456 matched within the age range for which the sedimentation is apparent, and the comparable
457 event deposits at the coring sites were named OW-4 to OW-20, thereby referencing the
458 deposit depth and facies characteristics (continuity of deposits that indicate thick layers).
459 Among these, event deposits OW-4 and OW-5 matched those identified as tsunami-
460 induced event deposits by Kase et al. (2016).
461 Among the event deposits interbedded in the cores, lateral changes in layer thickness
462 and particle size (Md and sorting) are shown in Figure 7 for deposits OW-4, -5, -8, -9, -
463 10, -12, -13, and -14, which are comparable in cores from three or more sites. In general,
464 sand layers with a thickness of 10 cm or more had different individual particle size
465 changes (as observed in the Md), but commonly exhibited upward fining. Sand layers that
466 were thick and could be divided into multiple units often exhibited upward fining in each
467 unit. The sorting of the sand layers and units with thicknesses of 10 cm and greater

468 occurred at many sites, with large variations. However, in some cases, the sorting tended
469 to worsen upward, owing to upward fining (Fig. 7).
470 Among the comparable event deposits, OW-5, OW-8, and OW-13 contained
471 sand layers that were thicker at the OKU-1 site near the coast and became thinner toward
472 the OKU-4 and OKU-5 sites on the landward side. Furthermore, the Md of core OKU-1
473 was 300-400 μm, but became 200–250 μm landward, indicating fining. In particular,
474 the Md of OW-13 in core OKU-5 underwent a sudden change in fining. Meanwhile, the
475 sorting of these event sand layers was ~2-3 in core OKU-1 and ~3 on the landward side,
476 indicating that sorting did not change as much as Md. In addition, the sorting became
477 slightly worse as the layers thinned and grains became finer landward. These changes
478 indicate that sorting may have worsened due to the incorporation of fine terrigenous
479 particles as they flowed upstream (inland). The sand layer in OW-14 has a thickness of
480 ~20 cm in core OKU-1, but became thicker in core OKU-3, and multiple units were
481 observed. The layer thickness decreased by half landward. The Md was 280–360 μm in
482 cores OKU-1 and OKU-3, suggesting upward fining. In contrast, the Md in cores OKU-
483 4 and OKU-5 sites were ~250–370 μm and 230–320 μm, respectively, and exhibited

484 slight fining. However, the upward fining in each unit was unclear, and large variations
485 were observed throughout. Sorting also tended to become poor, as large variations were
486 observed at the landward sites (Fig. 7).
487 Overall, for each event deposit, the layer thicknesses generally became thinner
488 and the grains tended to become finer landward. For reference, the Md of the sand layer
489 at the present beach (foreshore environment) of the Wasabiyachi lowland estuary is 270–
490 340 μm, which is similar to the Md of the event layers in cores OKU-1 and OKU-2 near
491 the coast. In addition, the sorting of the present beach sand is ~1.4, which is better sorted
492 than the event sand layers. The lack of uniform event deposit layer thicknesses and grain
493 sizes with distance from the ocean indicates differences due to water mass speed during
494 an event, as well as differences in water depth in the depositional area (microtopography
495 of a lagoon or floodplain).
496
497 ------Figure 7----
498
499 **5.4. Event deposit origin**

Kase et al. (2016) conducted hand boring and dug trial pits up to ~2 m in depth, obtaining event deposits at five horizons (Ow-1 to Ow-5). The characteristics of these event deposits included the following: 1) the layers become thinner and the grains become finer landward; 2) they had a grain size composition similar to that of beach sand; 3) the grain fabric of the sand layer indicated a landward paleo-flow direction; and 4) marine dinoflagellate cysts and foraminiferal linings were present in the sand layer. In addition, since the Wasabiyachi lowland has not experienced any flood damage from storm surges or tsunamis in the last 300 years, we can conclude that the origin of these event deposits was multiple tsunamis that occurred over time. Based on radiocarbon dating of the deposits, the age of Ow-1 was 0.7–1.0 ka, Ow-2 and Ow-3 were 1.7–1.9 ka, Ow-4 was ~2.6 ka, and Ow-5 was ~3.0 ka. Kawakami et al. (2017a, b) re-investigated the tsunami history of the entire Okushiri Island (including the Wasabiyachi lowland) and named the tsunami deposit caused by the sector collapse on Oshima-Oshima in 1741 as OK-1, Ow-1 of Kase et al. (2016) was named OK-2, Ow-2, and Ow-3 were named OK-3 (~1.5 ka), and Ow-4 and Ow-5 were named OK-4 and OK-5, respectively. OW-4 and OW-5 in the present study correspond to Ow-4 and Ow-5 in the Kase et al. (2016) study, and OK-4

516 and OK-5 in the Kawakami et al. (2017a, b) studies, respectively. Note that the
517 radiocarbon dating calculations conducted by Kase et al. (2016) were revised according
518 to IntCal 09 (Raimer et al., 2009), and have since been recalculated according to IntCal
519 20 (Raimer et al., 2020). As a result, the difference in the calibration ages (2σ) according
520 to IntCal 09 and IntCal 20 is approximately 10 to 80 years, which does not constitute a
521 major change to the chronological outline for Ow-1 to Ow-5 that was established
522 previously.

523 Overall, events deposits OW-6 to OW-20 exhibited thinner layers and finer
524 grains landward. In addition, the grain size composition of the sand layers interbedded at
525 seaward sites OKU-1 and OKU-2 were similar to those of the current beach sand. This
526 strongly suggests that the sand layers between OW-6 and OW-20 were derived from the
527 sea, and not inland regions. In addition, the sand layers of the lower deposits (OW-13 to
528 OW-20) were interbedded with the muddy sediment of an obstructed lagoon environment.
529 This lagoon deposit contains extremely thin laminated facies with no bioturbation,
530 indicating the presence of a closed lagoon in which sand layers that originated in the river
531 have not been transported. In contrast to this depositional environment, the sand layers

between OW-13 and OW-20 indicate that they were transported to the lagoon over the beach ridges that developed along the coast. The upper deposits (OW-6 to OW-12) are interbedded with peat layers and muddy lowlands in a similar manner to Ow-4 and Ow-5. The sand layers in these deposits (OW-6 to OW-12) have not been examined for marine microfossils, as in Kase et al. (2016). However, these sand layers were interbedded in a depositional environment in a similar manner to Ow-4 and Ow-5, suggesting that the process of sand layer formation was the same. Accordingly, it is likely that event deposits OW-6 to OW-20 observed in this study are tsunami deposits caused by tsunamis beyond the beach ridges that have been surmised to have been present between the Wasabiyachi lowland and the coast.

5.5. History of tsunami events and potential tsunami sources

Kase et al. (2016) and Kawakami et al. (2017a, b) surveyed tsunami deposits in the coastal lowlands of Okushiri Island and in the Hiyama region of Hokkaido. On Okushiri Island, five horizons (OKU-1 to OK-5) were observed in peat layers that are ~3,000 years old. Two horizons (HY-1 and HY-2) were also observed in the Hiyama

548 region. In addition, turbidite layers at four horizons (ST-1 to ST-4) were observed in the
549 Shiribeshi Trough off the coast of Hokkaido, which have been established as turbidites
550 that originated from an earthquake (Shimokawa and Ikehara, 2002). Among these, OK-
551 1, HY-1, and ST-1 are tsunami deposits that were caused by the sector collapse on
552 Oshima-Oshima in 1741 (Satake, 2007; Satake and Kato, 2001), whereas OK-2, HY-2,
553 and ST-2 are deposits caused by tsunamis ~800 years ago. In addition, it has been
554 suggested that OK-5 and ST-3 are sediments produced by a tsunami ~3,000 years ago.
555 According to previous studies, tsunami records in the Japan Sea off the southwestern
556 coast of Hokkaido contain only six horizons that extend to ~3–3.5 ka, including the ST-
557 4 event observed in the Shiribeshi Trough (~3.5 ka; Kawakami et al., 2017a, b).
558 Of these previously identified horizons, the tsunami event ~800 years ago may
559 have been generated by F17 or F18 in the fault model by the Committee of the Japan Sea
560 (2014), based on similarities with the distribution of sedimentation caused by the 1741
561 tsunami (Kawakami et al., 2017) and source fault estimates based on numerical
562 calculations (Ioki et al., 2019). Thus, few studies of tsunami occurrence and their source
563 faults have been conducted in the Japan Sea off the southwestern coast of Hokkaido.

564 In this study, we clarified the history of tsunami deposits on Okushiri Island
565 and extended the record to ~7.6 ka (Fig.3 and Table 3). Until now, tsunami records in the
566 northern Japan Sea from ~7 to 8 ka have only been observed in Lake Kamo, Sado Island,
567 Niigata Prefecture, and in the old Iwafune Lagoon in Murakami City, Niigata Prefecture
568 (Urabe, 2017). Future studies should compare the tsunami records and estimated tsunami
569 sources for Okushiri Island, Hokkaido, and Sado Island, Niigata Prefecture.
570
571 **6. Conclusions**
572 In this study, an extended coring survey was conducted in the Wasabiyachi
573 lowland on Okushiri Island, southeast of Hokkaido. Since beach ridges formed between
574 the Wasabiyachi lowland and the coast at ~8 ka, peaty lowland deposits have been
575 continuously deposited in closed lagoons. Such topographical/geological environments
576 are suitable for examining tsunami records that are much older than those researched to
577 date. As a result, 17 deposits (OW-4 to OW-20) produced by offshore tsunamis were
578 identified, and their ages were estimated. The results of this study can be used to
579 contribute to the tsunami occurrence history of the northern part of the Japan Sea and the

analysis of potential source faults located offshore of NE Japan.

Declarations

Ethics approval and consent to participate

Not applicable

Consent for publication

Not applicable

Availability of data and materials

Not applicable

Competing interests

There are no competing interests in relation with the present research.

Funding

596 This study was supported by “Integrated Research Project on Seismic and Tsunami
597 Hazards Around the Sea of Japan” of MEXT (Ministry of Education, Culture, Sports,
598 Science and Technology in Japan). (PI: Masanao Shinohara, Co-PI: Atsushi
599 Urabe).

600

601 **Authors' contributions**

602 AU and YK contributed to writing the main part of the paper and re-
603 correction of age dating. AU, YK, GK, and NK did geological survey and
604 borehole sampling. YT carried out grain size analysis and sedimentological
605 interpretations. HM and FH carried out grain size and total sulfur quantity
606 analyses.

607

608 **Acknowledgments**

609 The authors thank appreciate the officers of Okushiri town hall and
610 landowner of the study area.

611

612 ## References

613 Abe K, Ishii H. (1987) Distribution of maximum water levels due to the Japan Sea
614 Tsunami on 26 May 1983. J Oceanogr 43:169-182.
615 https://link.springer.com/article/10.1007/BF02109217.

616 Aomori Prefecture (1984) Record of disasters in the 1983 (Showa 58) Middle Japan Sea
617 Earthquake. Department firefighting and disaster prevention of Aomori Prefecture,
618 Aomori (In Japanese).

619 Bhattacharya JP, Walker RG, (1992) Deltas. In: Walker RG, James NP (eds.), Facies
620 Models: Response to Sea-Level Change. Geological Association of Canada, pp
621 157-177.

622 Committee for Technical Investigation on Large-Scale Earthquakes in the Japan Sea,
623 2014. Final report of committee.
624 https://www.mlit.go.jp/river/shinngikai_blog/daikibojishinchousa/houkoku/Repo
625 rt.pdf. Accessed 30 September 2021, (In Japanese).

626 Geological Survey of Hokkaido (1994) The ground disaster, tsunami disaster caused by
627 the 1993 Hokkaido-Nansei-Oki Earthquake. Research report of the Geological

628 Survey of Hokkaido. 24 (In Japanese).

629 Hata M, Segawa S, Yajima J (1982) Geology of the Okushirito hokubu and nanbu district.

630 Quadrangle Series, scale 1:50,000. Geological Survey of Japan (in Japanese with

631 English abstract).

632 Heaton JT, Köhler P, Butzin M, Bard E, Reimer WR, Austin ENW, Bronk Ramsey C,

633 Grootes MP, Hughen A, Kromer B, Reimer JP, Adkins J, Burke A, Cook SM,

634 Olsen J, Skinner CM (2020) Marine20 – the marine radiocarbon age calibration

635 curve (0-55,000). Radiocarbon:62, 779-820.

636 https://doi.org/10.1017/RDC.2020.68.

637 Hokkaido archaeological operations center (2002) Report of Hokkaido archaeological

638 operations center, part 2: Aonae dune site. Hokkaido archaeological operations

639 center, Sapporo.

640 Ioki K, Tanioka Y, Kawakami G, Kase Y, Nishina K, Hirose W, Hayashi K, Takahashi

641 R (2019) Fault model of the 12th century southwestern Hokkaido earthquake

642 estimated from tsunami deposit distributions. Earth Planets and Space:71, 54.

643 https://doi.org/10.1186/s40623-019-1034-6.

644 Isozaki Y, Aoki K, Nakama T, Yanai S, (2010) New insight into a subduction-related
645 orogen: a reappraisal of the geotectonic framework and evolution of the Japanese
646 Islands. Gondwana Res:18, 82-105. https://doi.org/10.1016/j.gr.2010.02.015.1
647 Japan Meteorological Agency (1984) The report on the Nihonkai-Chubu earthquake,
648 1983. Technical report of Japan Meteorological Agency:106, 1-252 (In Japanese).
649 Japan Meteorological Agency (1995) Report on the Hokkaido-Nansei-Oki earthquake,
650 1993. Technical report of Japan Meteorological Agency:117, 1-281 (In Japanese).
651 Japan Meteorological Agency (2012) Report on the 2011 off the pacific coast of Tohoku
652 earthquake, 1993. Technical report of Japan Meteorological Agency:133, 1-479
653 (In Japanese).
654 Kamataki T, Abe N, Kanazawa S, Matsutomi H (2017) A study on paleo-tsunami
655 inundation area and deposits in coastal lowland on the southern part of Akita
656 Prefecture, the eastern margin of Japan Sea. J Japan Soc Civil Eng Ser B2 (Coastal
657 Eng): 73, I_445-I_450. https://doi.org/10.2208/kaigan.73.I_445 (In Japanese with
658 English abstract).
659 Kamataki T, Abe K, Kurosawa K, Miwa A, Imamura T (2015) Event deposits recorded

660 in coastal lowland on the western coast of the Akita Prefecture, the eastern margin
661 of Japan Sea. The Quatern Res (Daiyonki-Kenkyu):54, 129-138.
662 https://doi.org/10.4116/jaqua.54.129 (In Japanese with English abstract).
663 Kamataki T, Matsutomi H, Umeda K, Abe K, Kurosawa H (2018a) Event deposits and
664 their depositional ages recorded in coastal lowland along the eastern margin of the
665 Japan Sea. Tohoku J Nat Dis Sci:54, 55-60 (In Japanese with English abstract).
666 Kamataki T, Takabuchi S, Matsutomi H, Abe K, Kurosawa H (2016) A study on tsunami
667 deposits in coastal lowland on the middle-northern part of Akita Prefecture, the
668 eastern margin of Japan Sea. J Japan Soc Civil Eng Ser B2 (Coastal Eng):72,
669 I_1693-I_1698. https://doi.org/10.2208/kaigan.72.I_1693 (In Japanese with
670 English abstract).
671 Kamataki T, Uchidate M, Kanazawa S, Ishida M, Matsutomi H (2018b) A study of paleo-
672 tsunami history around the area affected by the 1983 Japan Sea Earthquake,
673 coastal lowland on the northern part of Akita Prefecture, the eastern margin of
674 Japan Sea. J Japan Soc Civil Eng Ser B2 (Coastal Eng):74, I_529 – I_534.
675 https://doi.org/10.2208/kaigan.74.I_529 (In Japanese with English abstract) .

676 Kamataki T, Unai H, Tokumaru T, Matsutomi H (2019) A study of paleo-tsunami history
677 in coastal lowland on the southern part of Yamagata and northern part of Akita
678 Prefectures, the eastern margin of Japan Sea. J Japan Soc Civil Eng Ser B2
679 (Coastal Eng):75, I_403-I_408. https://doi.org/10.2208/kaigan.75.I_403 (In
680 Japanese with English abstract).
681 Kawakami G, Nishina K, Kase Y, Hirose W, Tajika J, Watanabe T, Ishimaru S, Sagayama
682 T, Hayashi K, Takahashi R, Fukami K, Tamura S, Koshimizu K, Okazaki N,
683 Ohtsu S (2015) Geological records of tsunamis along the coasts of the Japan Sea
684 and the Okhotsk Sea in Hokkaido, Japan. Special Report, Geological Survey of
685 Hokkaido:42, 1-218 (In Japanese with English abstract).
686 Kawakami G, Kase Y, Urabe A, Takashimizu Y, Nishina K, (2017a) Tsunamis and
687 possible tsunamigenic deposits along the eastern margin of the Japan Sea. J Geol
688 Soc Japan:123, 857-877. https://doi.org/10.5575/geosoc.2017.0054 (In Japanese
689 with English abstract).
690 Kawakami G, Nishina K, Kase Y, Tajika J, Hayashi K, Hirose W, Sagayama T, Watanabe
691 T, Ishimaru S, Koshimizu K, Takahashi R, Hirakawa K (2017b) Stratigraphic

692 records of tsunamis along the Japan Sea, southwest Hokkaido, northern Japan.
693 Island Arc:26, e12197, https://doi.org/10.1111/iar.12197.
694 Koike K, Machida H (2001) Atlas of quaternary marine terraces in the Japanese islands.
695 Univ. Tokyo Press, Tokyo (In Japanese).
696 Miall AD (1992) Alluvial deposits. In: Walker RG, James NP (eds.), Facies Models:
697 Response to Sea Level Change. Geological Association of Canada, Waterloo,
698 Ontario. pp.119-139.
699 Minoura K, Nakaya S (1990) Origin of Inter-Tidal Lake and Marsh Environments in and
700 around Lake Jusan, Tsugaru. Mem Geol Soc Japan:36, 71-87 (In Japanese with
701 English abstract).
702 Minoura K, Nakaya S (1991) Traces of tsunami preserved in inter-tidal lacustrine and
703 marsh deposits: some examples from Northeast Japan. J Geology:99, 265-287.
704 https://doi.org/10.1086/629488.
705 Minoura K, Nakaya S, Sato H (1987) Traces of Tsunamis Recorded in Lake Deposits -
706 An Example from Jusan, Ichiura-mura, Aomori-. J Seismo Soc Japan Sec Series
707 40:183-196. https://doi.org/10.4294/zisin1948.40.2_183 (In Japanese with

English abstract).

Miyoshi M, Ota Y, Sawa H, Imaizumi T, Kashima K (1985) Holocene marine terraces of Okushiri island, off the western Hokkaido, Japan. Geographical Review of Japan Ser A:58, 596-608. https://doi.org/10.4157/grj1984a.58.9_596 (In Japanese with English abstract).

Nanayama F, Shigeno K, Satake K, Shimokawa K, Koitabashi S, Miyasaka S, Ishii M (2000) Sedimentary differences between the 1993 Hokkaido-nanseioki tsunami and the 1959 Miyakojima typhoon at Taisei, southwestern Hokkaido, northern Japan. Sediment Geol:135, 255-264. https://doi.org/10.1016/S0037-0738(00)00076-2.

Nishimura Y, Miyaji N, Yoshida M (1999) Survey of tsunami deposit along the western coast of north Hokkaido, Japan. Historical Earthquake:15, 255-231 (In Japanese with English abstract).

Nishimura Y, Suzuki M, Miyaji N, Yoshida M, Murata D (2000) Deposit of historical tsunami identified at Ayukawa coast, Kumaishi, Oshima Peninsula, Hokkaido. Chikyu Monthly (Special issue):82, 147-153 (In Japanese).

724 Okada R, Kaji J, Umeda K, Kamataki T, Ishida M, Uchidate M (2018) Event deposits
725 recorded the Lake Jusanko, Tsugaru Peninsula. Tohoku J Nat Disas Sci:54, 49-54
726 (In Japanese with English abstract).
727 Okada R, Umeda K, Kamataki T (2019) Traces of tsunami and liquefaction recorded
728 around the Lake Jusan, Tsugaru Peninsula. Tohoku J Nat Disas Sci:55, 25-30 (In
729 Japanese with English abstract).
730 Okamura Y (2000) Inversion tectonics along the eastern margin of the Japan Sea, J Japan
731 Assoc Petro Tech:65, 40-47, https://doi.org/10.3720/japt.65.40 (In Japanese with
732 English abstract).
733 Okamura Y (2010) Relationship between geological structure and earthquake source
734 faults along the eastern margin of the Japan Sea. Journal of the Geological Society
735 of Japan:116, 582-591. https://doi.org/10.5575/geosoc.116.582 (In Japanese with
736 English abstract).
737 Reimer PJ, Austin WEN, Bard E, Bayliss A, Blackwell PG, Bronk Ramsey C, Butzin M,
738 Cheng H, Edwards RL, Friedrich M, Grootes PM, Guilderson TP, Hajdas I,
739 Heaton TJ, Hogg AG, Hughen KA, Kromer B, Manning SW, Muscheler R,

740 Palmer JG, Pearson C, van der Plicht J, Reimer RW, Richards DA, Scott EM,
741 Southon JR, Turney CSM, Wacker L, Adolphi F, Büntgen U, Capano M, Fahrni
742 SM, Fogtmann-Schulz A, Friedrich R, Köhler P, Kudsk S, Miyake F, Olsen J,
743 Reinig F, Sakamoto M, Sookdeo A, Talamo S (2020) The IntCal20 northern
744 hemisphere radiocarbon age calibration curve (0–55 cal kBP). Radiocarbon:62,
745 725-757. https://doi.org/10.1017/RDC.2020.41.
746 Reimer PJ, Baillie MGL, Bard E, Bayliss A, Beck JW, Blackwell PG, Bronk Ramsey C,
747 Buck CE, Burr GS, Edwards RL, Friedrich M, Grootes PM, Guilderson TP,
748 Hajdas I, Heaton TJ, Hogg AG, Hughen KA, Kaiser KF, Kromer B, McCormac
749 FG, Manning SW, Reimer RW, Richards DA, Southon JR, Talamo S, Turney
750 CSM, van der Plicht J, Weyhenmeyer CE (2009) IntCal09 and Marine09
751 Radiocarbon Age Calibration Curves, 0–50,000 Years cal BP. Radiocarbon:51,
752 1111-1150. https://doi.org/10.1017/S0033822200034202.
753 Reinson GE (1984) Barrier-island and associated strand-plain systems. In: Walker RG
754 (ed.) Facies Models. Geological Association of Canada, Geoscience Canada
755 Reprint Series 1, St. John's, Hamilton, Canada, pp 119-140.

Satake K (2007) Volcanic origin of the 1741 Oshima-Oshima tsunami in the Japan Sea. Earth Planet and Space:59, 381-390. https://doi.org/10.1186/BF03352698.

Satake K, Kato Y (2001) The 1741 Oshima-Oshima eruption: extent and volume of submarine debris avalanche. Geophys Res Lett:28, 427-430. https://doi.org/10.1029/2000GL012175.

Seno T (1999) Syntheses of the regional stress fields of the Japanese islands. Island Arc:8, 66-79. https://doi.org/10.1046/j.1440-1738.1999.00225.x.

Seno T, Sakurai T, Stein S (1996) Can the Okhotsk Plate be discriminated from the North American Plate? J Geophys Res Solid Earth:101, 1305-11315. https://doi.org/10.1029/96JB00532.

Shimokawa K, Ikehara K (2002) Chapter 6, The paleo-earthquake recorded to sediment. In: Otake M, Taira A, Ota Y (eds) Active faults and seismo-tectonics of the eastern margin of the Japan Sea. Tokyo University Press, Tokyo. pp. 95-108 (In Japanese).

Shuto N (1984) Trace highs of tsunami of the Japan Sea Earthquake of 1983. Report of tsunami laboratory, Tohoku Univ:1, 88-267 (In Japanese).

Strum M (1979) Origin and composition of clastic varves. In: Schlucher C (ed.) Moraines

772 and Varves: Origin, Genesis, Classification, CRC Press, Rotterdam, pp 281-285.
773 Taira A (2002) Active Faults and Seismo-Tectonics of the Eastern Margin of the Japan
774 Sea. In: Otake M, Taira A, Ota Y (eds) Active faults and seismo-tectonics of the
775 eastern margin of the Japan Sea. Tokyo University Press, Tokyo. pp 38-61 (In
776 Japanese).
777 Takashimizu Y, Kawakami G, Urabe A (2020) Tsunamis caused by offshore active faults
778 and their deposits. Earth-Sci Rev:211, 103380.
779 https://doi.org/10.1016/j.earscirev.2020.103380.
780 Urabe A (2017) Reconstruction of tsunami history based on event deposits in the Niigata
781 area, eastern coast of the Sea of Japan. Quart Int:456, 53-68.
782 https://doi.org/10.1016/j.quaint.2017.05.045.
783 Urabe A (2019) Examination of tsunami history based on the sediment survey in the Japan
784 Sea side, South-West Japan. Report of the Coordinating Committee for
785 Earthquake Prediction Japan:102, 420-421 (In Japanese).
786

Figure and table captions

Figure 1 Distribution of the active faults in the offshore between Aomori to Hokkaido, northern part of Japan Sea (Committee for Technical Investigation on Large-Scale Earthquakes in the Sea of Japan, 2014). Okushiri island is located at the offshore of southwest Hokkaido, and active faults is distributed over the surrounding sea. Lage earthquake (1983 Middle Japan Sea earthquake and 1993 Hokkaido Nansei-Oki earthquake) occurred in this area.

Figure 2 Topography around the Wasabiyachi lowland, Aonae region, southern part of Okushiri island. Index map shows the localities of borehole sites. Geologic and geomorphologic classification of landforms is based on Hata et al. (1982) and Koike and Mchida (2001). The Wasabiyachi lowland along the Aonae Bay is barriered by Holocene marine terrace and coastal beach ridge with sand dune. Contour maps are reproduced from online map of the Geospatial Information Authority of Japan (GSJ).

803 Figure 3 Geological log of the OKU-1 - OKU-5 cores, 14C ages and event deposits.
804 Seventeen event deposits (tsunami sand beds: OW-4 – OW-20) are well correlated
805 in the Wasabiyachi lowland (see Figure 2 for location).
806
807 Figure 4 Vertical changes of grain size analysis and content of total sulfur of the OKU-
808 3 core. The grain size analysis showed Md (median grain size), G.M. (geometric
809 mean grain size), Mo (mode grain size) and sorting (geometric standard deviation)
810 in the figure.
811
812 Figure 5 Age-depth curve of the OKU-1 – OKU-5 cores with estimated ages of event
813 deposits. The vertical axis of the graph shows the depth and thickness of event
814 deposits. The horizontal axis shows the calibrated age value to clearly indicate the
815 correlation of the event deposits.
816
817 Figure 6 Photograph of lithofacies and event deposits in depth 0 – 15 m of the OKU-3
818 core. The event deposits are consisted of well-sorted sand layer. The lithofacies of

819 event deposits are clearly different from the steady depositional environment.
820 The facies code of LG2 and LG3 show laminated silt and clay-silt of occlusive
821 lagoon. The FL4 and FL5 show peaty environment of fluvial floodplain. The Ko-d
822 (AD 1640 Komagatake-d tephra) is widely distributed in the southern part of
823 Hokkaido, and this tephra is compared in the Okushiri area (Kase et al. 2016 and
824 Kawakami et al. 2017a).
825
826 Figure 7 Stratigraphic correlation and changes of lithofacies, Md (median grain size),
827 and sorting (geometric standard deviation) of the event deposits (OW-4, -5, -8, -9,
828 -10, -12, -13, and -14).
829
830 Table 1 ^{14}C age summary of the OKU-1 to OKU-5 cores. Age ranges are calibrated
831 using IntCal 20 and Marine 20.
832
833 Table 2 ^{14}C age dating of the Wasabiyachi lowland reported by Kase et al. (2016). Kase
834 et al. (2016) carried out the age calibration using IntCal 09. In this study, the ^{14}C

835 ages carried out re-calibration using IntCal 20.

836

837 Table 3 Description of lithofacies and estimated age of the event deposits for the OKU-

838 1 to OKU-5.

Figures

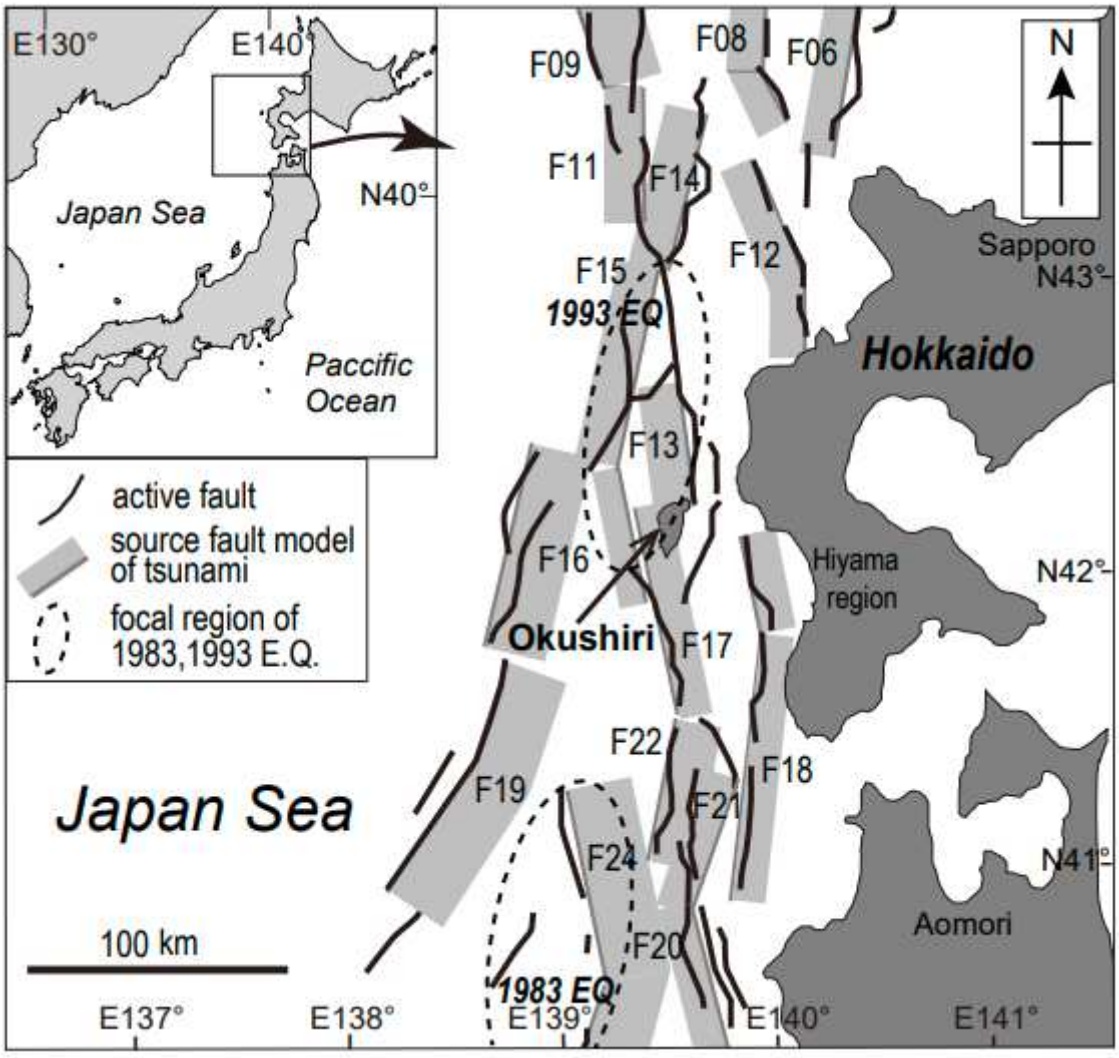

Figure 1

Distribution of the active faults in the offshore between Aomori to Hokkaido, northern part of Japan Sea (Committee for Technical Investigation on Large-Scale Earthquakes in the Sea of Japan, 2014). Okushiri island is located at the offshore of southwest Hokkaido, and active faults is distributed over the surrounding sea. Lage earthquake (1983 Middle Japan Sea earthquake and 1993 Hokkaido Nansei□793 Oki earthquake) occurred in this area.

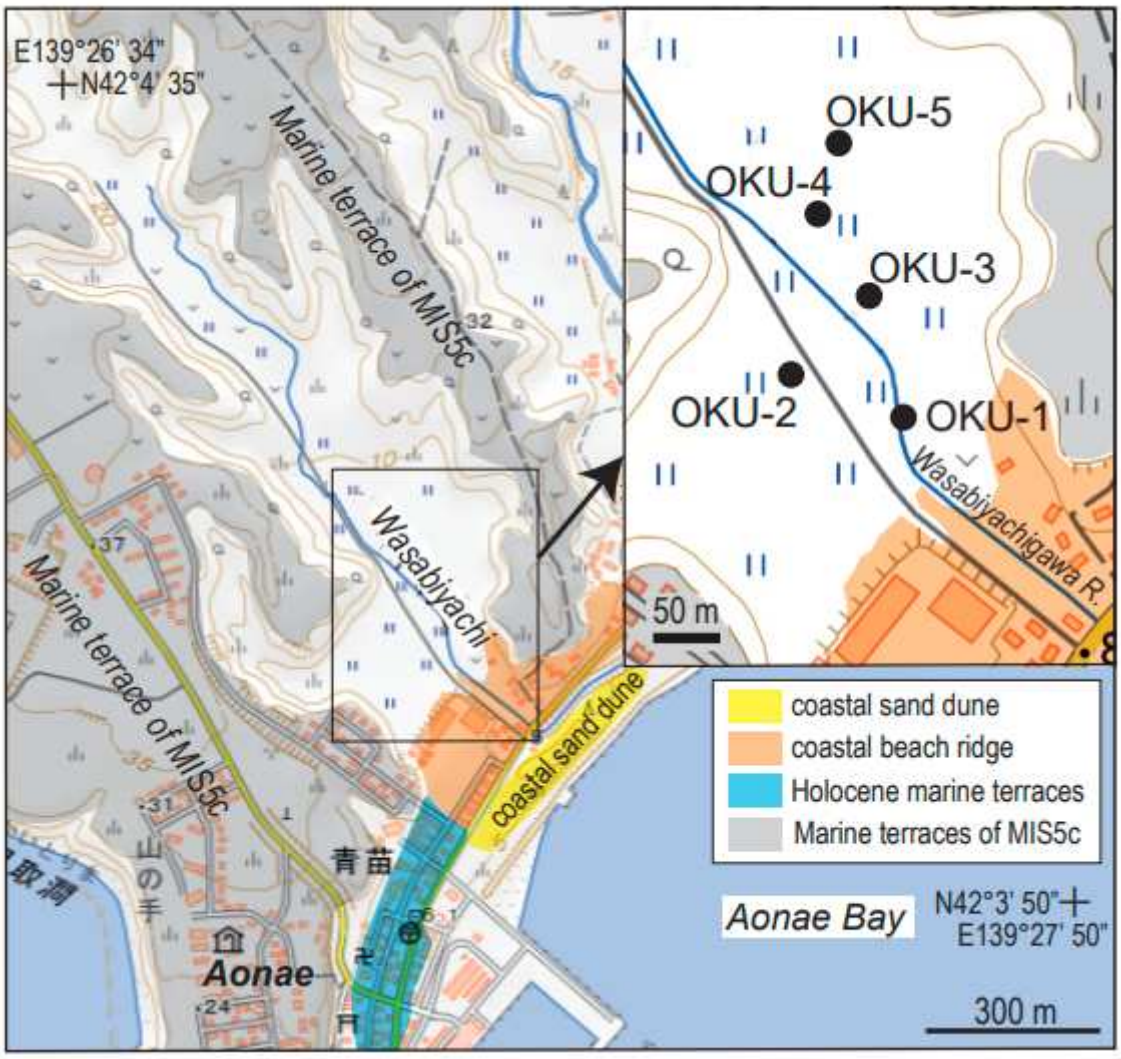

Figure 2

Topography around the Wasabiyachi lowland, Aonae region, southern part of Okushiri island. Index map shows the localities of borehole sites. Geologic and geomorphologic classification of landforms is based on Hata et al. (1982) and Koike and Mchida (2001). The Wasabiyachi lowland along the Aonae Bay is barriered by Holocene marine terrace and coastal beach ridge with sand dune. Contour maps are reproduced from online map of the Geospatial Information Authority of Japan (GSJ).

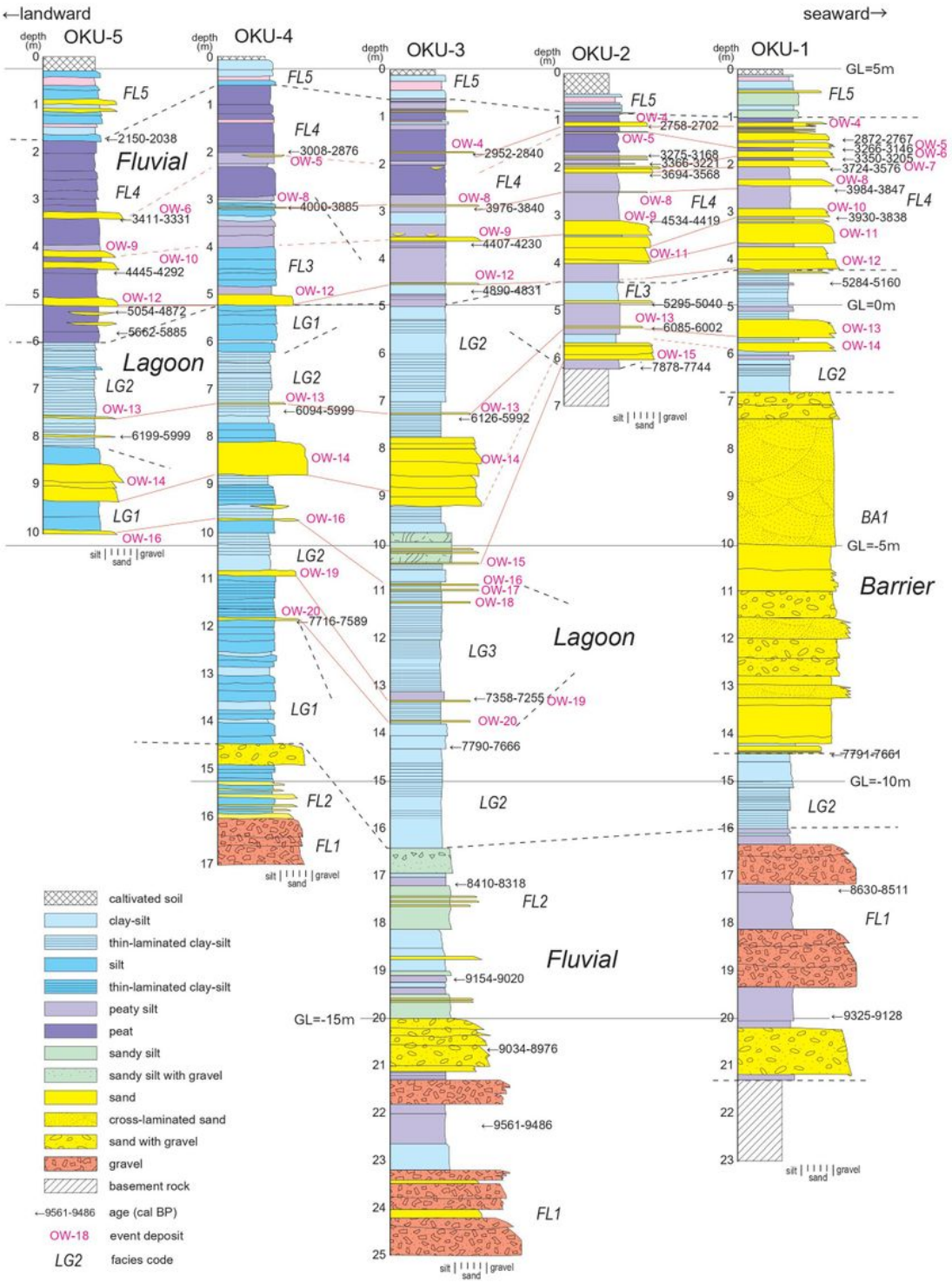

Figure 3

Geological log of the OKU-1 - OKU-5 cores, 14C ages and event deposits. Seventeen event deposits (tsunami sand beds: OW-4 – OW-20) are well correlated in the Wasabiyachi lowland (see Figure 2 for location).

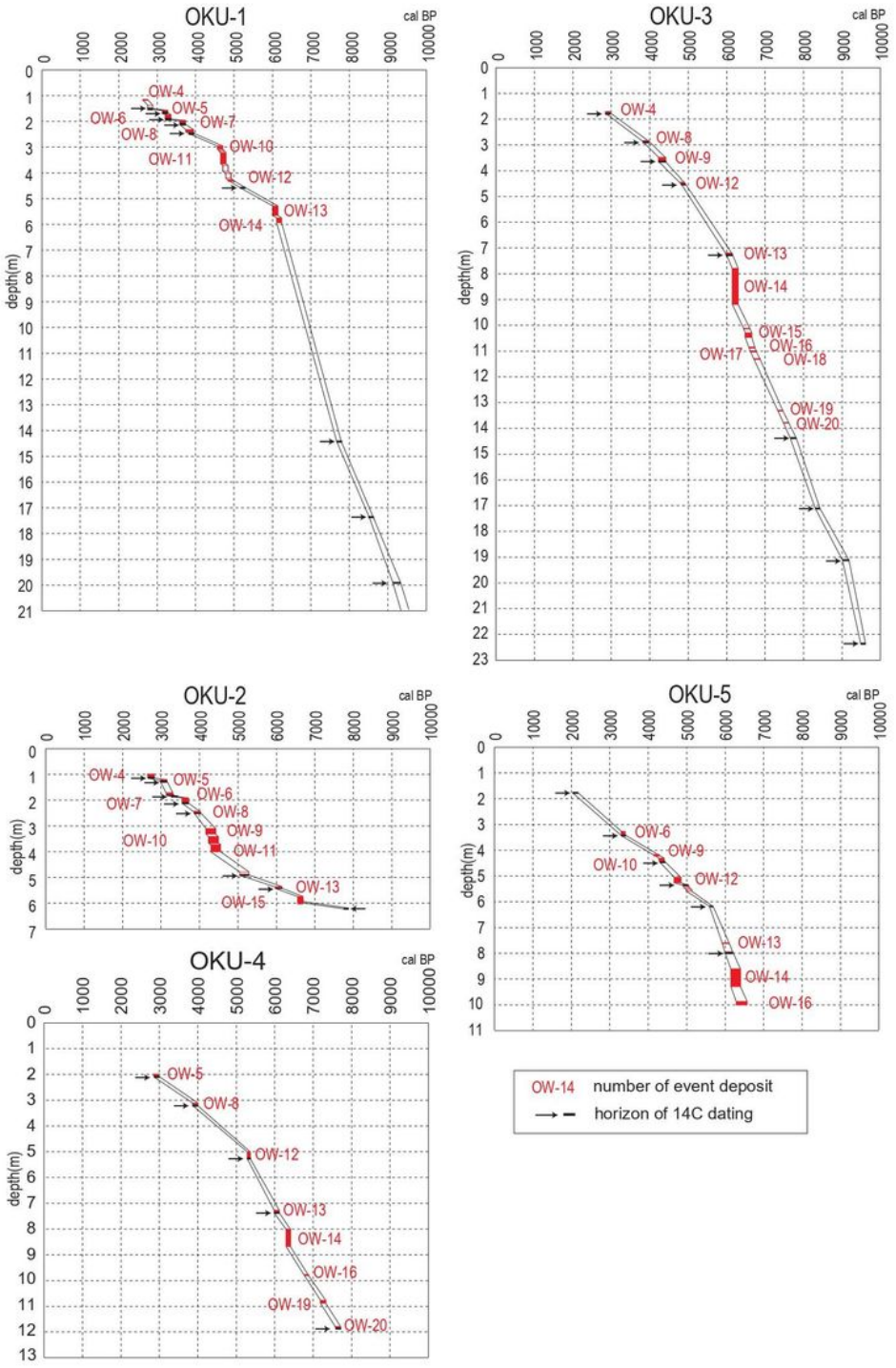

Figure 4

Vertical changes of grain size analysis and content of total sulfur of the OKU-3 core. The grain size analysis showed Md (median grain size), G.M. (geometric mean grain size), Mo (mode grain size) and sorting (geometric standard deviation) in the figure.

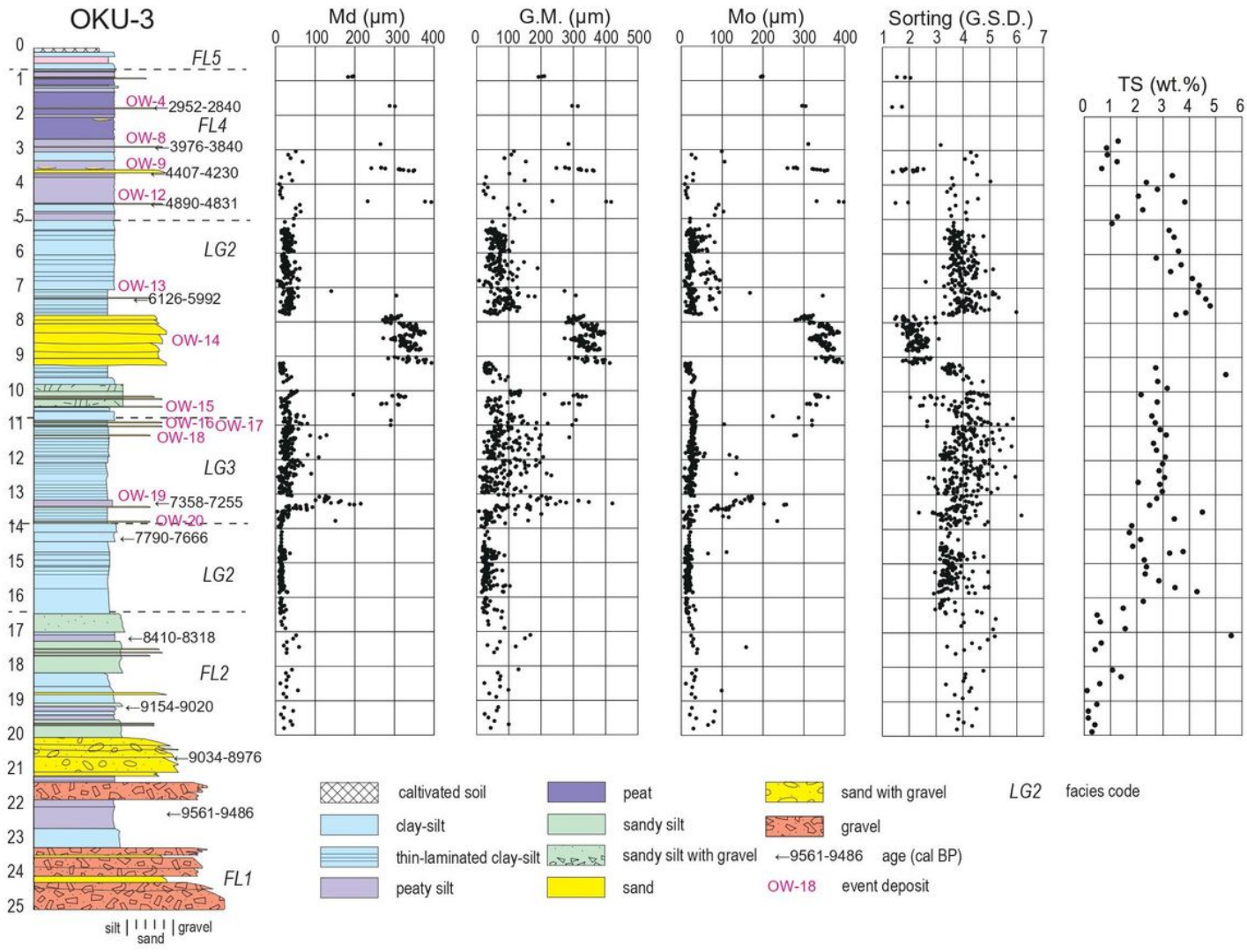

Figure 5

Age-depth curve of the OKU-1 – OKU-5 cores with estimated ages of event deposits. The vertical axis of the graph shows the depth and thickness of event deposits. The horizontal axis shows the calibrated age value to clearly indicate the correlation of the event deposits.

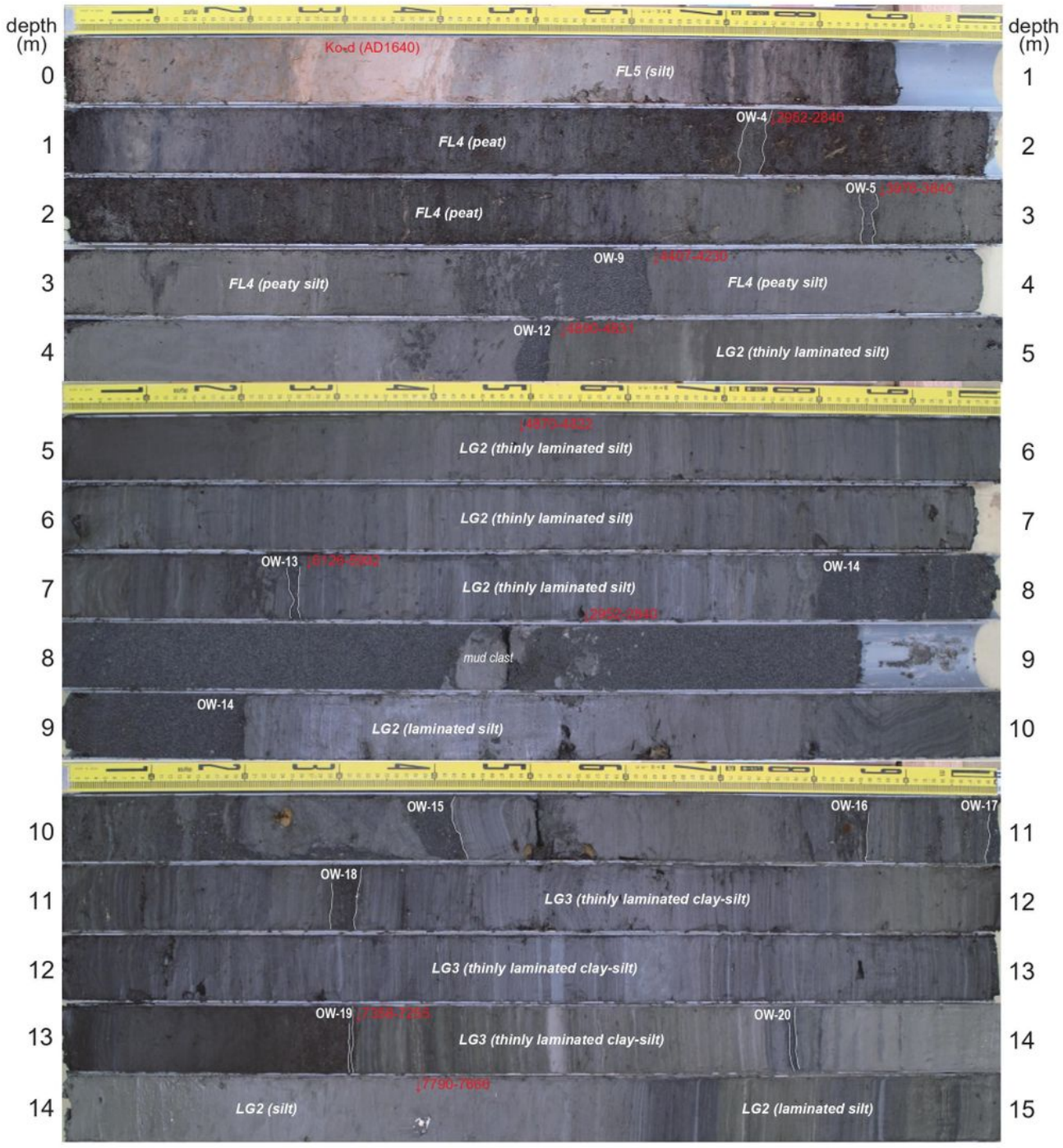

Figure 6

Photograph of lithofacies and event deposits in depth 0 – 15 m of the OKU-3 core. The event deposits are consisted of well-sorted sand layer. The lithofacies of event deposits are clearly different from the steady depositional environment. The facies code of LG2 and LG3 show laminated silt and clay-silt of occlusive lagoon. The FL4 and FL5 show peaty environment of fluvial floodplain. The Ko-d (AD 1640 Komagatake-

d tephra) is widely distributed in the southern part of Hokkaido, and this tephra is compared in the Okushiri area (Kase et al. 2016 and Kawakami et al. 2017a).

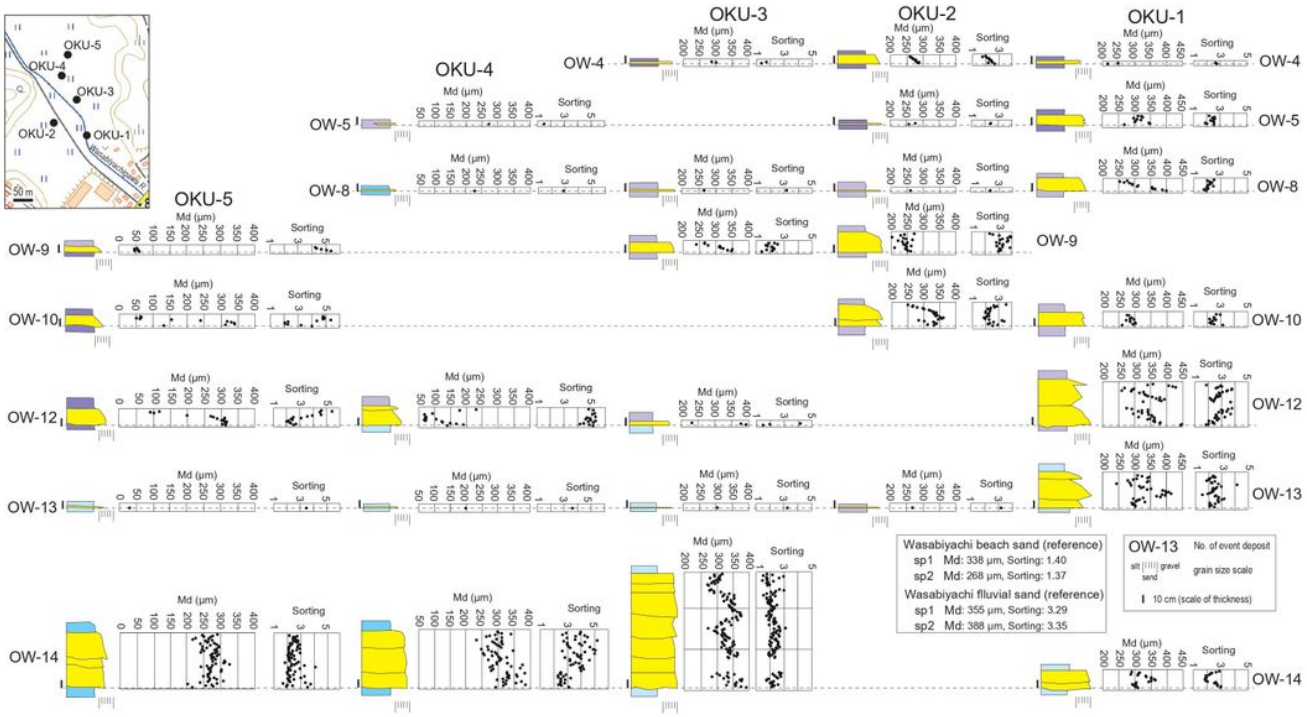

Figure 7

Stratigraphic correlation and changes of lithofacies, Md (median grain size), and sorting (geometric standard deviation) of the event deposits (OW-4, -5, -8, -9, -10, -12, -13, and -14).

Supplementary Files

This is a list of supplementary files associated with this preprint. Click to download.

- Table1urabe.xlsx
- Table2urabe.xlsx
- Table3urabe.xlsx
- graabst.jpg